Phase diagrams of aligned dipolar hard rods

P. I. C. Teixeira*
FOM Instituut voor Atoom-en Molecuulfysica, Kruislaan 407, NL-1098 SJ Amsterdam, The Netherlands

M. A. Osipov† and M. M. Telo da Gama
Departamento de Física, Faculdade de Ciências da Universidade de Lisboa and Centro de Física da Matéria Condensada, Avenida Professor Gama Pinto 2, P-1699 Lisbon Codex, Portugal

(Received 3 September 1997)

Perfectly aligned, long dipolar hard rods are shown to exhibit unusual phase behavior, induced by the long range of the dipolar interaction in combination with the finite length of the particles. Three variants have been considered: (i) ellipsoids with central dipoles, (ii) spherocylinders with central dipoles, and (iii) spherocylinders with dipoles placed at regular intervals along their axes. In all cases, the dipoles are taken to be pointlike and directed longitudinally. At sufficiently low temperatures, coexistence between fairly low-density phases of similar structure has been found, which terminates at a critical point. Our results shed some light on recent simulations of dipolar soft spheres in a strong field, which separate into two ''gas'' phases of ordered, rodlike chains: Accord is semiquantitative in case (iii) and qualitative in cases (i) and (ii). Relaxing the assumptions of perfect order and molecular rigidity worsens agreement somewhat, but otherwise leads to no substantial changes. Possible refinements of the theory are discussed. [S1063-651X(98)12702-2]

PACS number(s): 61.20.Gy, 75.50.Mm, 64.70.−p

I. INTRODUCTION

One might reasonably expect that after more than 40 years of intense research into the structure of classical fluids, at least the phase behavior of the most basic models thereof should have been fully understood. That this is not the case has been amply demonstrated by the recent spate of interest in the demixing of hard spheres [1,2] and hard rods [3–7], as well as in the mechanisms whereby the range of the attractive part of the intermolecular potential can stabilize different phase equilibria in simple liquids [8–13].

However informative hard bodies may be, they by no means exhaust the abundant issue of nature's design or of human ingenuity. Indeed, just as common as the short-ranged overlap forces that they mimic is electric charge and hence multipole moments. The interaction between (even permanent point) dipoles is highly complex. This is a consequence of (i) its *long range*, which produces subtle effects relating to system size and the nature of the boundary conditions [14–19], and (ii) its very pronounced *anisotropy* and especially the strong coupling between the orientations of a pair of dipoles and that of the interdipole vector: Two parallel dipoles will repel each other if placed side by side but attract each other if head to tail.

It follows that the phase diagram of dipolar fluids in general and of *strongly* dipolar fluids in particular has remained largely uncharted. In 1970 de Gennes and Pincus [20] argued, on the basis of Keesom's Boltzmann-averaged, effective (isotropic) interdipole potential [21], that a system of hard particles with embedded dipoles should exhibit liquid-vapor (LV) coexistence identical to that due to dispersion interactions. Most subsequent theoretical treatments made the same prediction [22–30], which seemed to be confirmed by early simulation evidence [31]. Recent numerical work, however, has failed to find LV equilibria for either dipolar hard spheres (DHSs) or dipolar soft spheres (DSSs) [32–34]. Instead, at low densities dipoles tend to associate into chains akin to living polymers [33–36]. That they should do so can be readily understood in terms of the structure of the full, angle-dependent, dipole-dipole potential: The head-to-tail geometry is actually the most favorable, with an energy minimum twice as deep as that of the next-most-favorable configuration, namely, two antiparallel dipoles. For sufficiently large dipole moments, this difference gives rise to very anisotropic short-range correlations, whence comes chaining [37–39]. It is precisely such strong short-range correlations, present even at low densities, that are missed when one performs angular averages of the potential, as is done, in one form or another, in most theories (see [39] for a more detailed discussion of these difficulties and how they might be overcome). The discrepancy between old and new simulation results, on the other hand, has been ascribed to the smallness of the system simulated earlier [40].

Because strongly dipolar spheres form chains and interchain interactions of dipolar origin are very weak [39], some additional attraction between spheres is required to promote LV coexistence. Indeed, van Leeuwen and Smit have shown [33] that ''conventional'' behavior can be recovered by adding an isotropic attractive term to the DSS potential. They simulated a variant of the Stockmayer potential, with a variable ratio ϵ_6 of the strengths of the attractive and repulsive parts of the Lennard-Jones component; $\epsilon_6=0$ corresponds to a DSS and $\epsilon_6=1$ to the usual Stockmayer fluid. In zero field, LV phase coexistence and no chains were found for $\epsilon_6 \gtrsim 0.3$. Later, Stevens and Grest [41] mapped out the LV

*Present address: Cavendish Laboratory, Madingley Road, Cambridge CB3 0HE, United Kingdom.

†Permanent address: Institute of Crystallography, Russian Academy of Sciences, Leninski Prospekt 59, 117 333 Moscow, Russia.

phase diagram of (moderately polar) Stockmayer fluids with or without an applied field.

A minimum amount of isotropic attractive energy thus appears necessary to stabilize equilibria between isotropic phases in zero field, at least in three dimensions [33,34,41]. (Whether the same effect is present in a quasi-two-dimensional model, remains an open question [42].) Yet there are other ways to inhibit chain formation while retaining the basic model of a repulsive hard or soft core plus dipolar interaction. The simplest of these is to decrease the depth of the head-to-tail energy minimum relative to that corresponding to antiparallel dipoles by stretching the sphere into a rod along the direction of the dipole moment. McGrother and Jackson [43] have simulated a fluid of dipolar hard spherocylinders and found an island of LV coexistence when the two minima are nearly equal, i.e., for length-to-breadth ratios $0.19 \lesssim L/D \lesssim 0.27$ (they are equal for $L/D = 2^{1/3} - 1 \approx 0.26$) [44]. Longer spherocylinders again form chains, or rather ''ribbons,'' where nearest neighbors are now approximately antiparallel. This suggests that once chaining is suppressed by making the interaction potential ''less anisotropic,'' phase separation comes into play (a more detailed investigation of the competition between phase separation and aggregation in the DHS fluid is reported in [45]).

Coexistence between low-density phases of *ordered* DSS chains without additional attraction does nonetheless obtain if a strong field is applied [46]. This phase separation is very unusual is several ways. First, in contrast to LV equilibria, the (reduced) densities of the two phases are close and very low, $\rho^* \sim 0.02 - 0.03$. Moreover, their structures are also similar and resemble a gas of fairly ordered dipole chains. We propose that the behavior of such a system can be qualitatively understood using a simple model of long dipolar rods. A dipolar chain in a strong field is similar to a rod (with some flexibility perhaps) with dipoles distributed along its axis. Thus we arrive at the simplest model of perfectly aligned dipolar hard rods that still preserves the main qualitative features of the actual system of ordered dipole chains.

Now let us consider the possibility of phase separation in a fluid of strongly dipolar rods in a strong external field. As mentioned above, without a field the rods form ribbons with antiparallel nearest neighbors. However, there will be a critical field that destroys the ribbons because even at short distances the interaction between two antiparallel dipoles will be weaker than that of each of them with the field. Furthermore, if the rods are long enough, the head-to-tail minimum can be made very weak, even for very strong dipoles. Hence long polar rods do not form any chains or ribbons in a sufficiently strong external field. It will be shown below that in this case and under appropriate boundary conditions, the long-range character of the dipole-dipole interaction gives rise to an effective attraction between rods that depends on particle shape [47] and could be the driving force of the instability of the homogeneous fluid relative to two phases of aligned rods. Clearly, the effect should be qualitatively the same for all rod shapes and all distributions of (longitudinal) dipoles therein, but as we shall see, quantitative differences can be important. We argue that the same effect should be present in the system of ordered dipole chains.

In this paper we investigate the above scenario and discuss its relevance to the phase separation of the DSS fluid in an applied field. In Sec. II we present our theory and stress the need for a correct choice of boundary conditions when dealing with electrostatic forces. Section III contains our results for the fluid phase equilibria of (i) hard ellipsoids with central dipoles, (ii) hard spherocylinders with central dipoles, and (iii) hard spherocylinders with equispaced dipoles along their long axes: Although the qualitative picture is the same in all three cases, there are important quantitative differences. In particular, we shall argue that (iii) is relevant to the problem of the phase behavior of DSSs in a field and that relaxing the assumptions of perfect orientational order and infinite particle rigidity leads to no substantial changes. Finally, in Sec. IV we conclude with some critical remarks on our models and approach, as well as their relation to real ferrofluids.

II. THEORY

A. General formulation

The interaction potential between two point dipoles embedded in hard rods (HRs) is

$$\phi(\mathbf{x}_1,\mathbf{x}_2) = \phi_{\mathrm{ref}}(\mathbf{x}_1,\mathbf{x}_2) + \phi_{dd}(\mathbf{x}_1,\mathbf{x}_2), \tag{1}$$

where $\mathbf{x}_i$ denotes the set of position $\mathbf{r}_i$ and orientation $\mathbf{a}_i$ coordinates of particle i, $\phi_{\mathrm{ref}}(\mathbf{x}_1,\mathbf{x}_2)$ is a short-ranged reference potential incorporating the effects of steric repulsion, and

$$\phi_{dd}(\mathbf{x}_1,\mathbf{x}_2) = \begin{cases} -\dfrac{m^2}{r_{12}^3}[3(\hat{\mathbf{m}}_1\cdot\mathbf{u}_{12})(\hat{\mathbf{m}}_2\cdot\mathbf{u}_{12}) - \hat{\mathbf{m}}_1\cdot\hat{\mathbf{m}}_2] & \text{if } r_{12} \notin V_{\mathrm{exc}}(\omega_1,\omega_2) \\ 0 \quad \text{otherwise} \end{cases} \tag{2}$$

is the dipole-dipole interaction [48]. In Eq. (2), $\hat{\mathbf{m}}_i = \mathbf{m}_i/m$ is a unit vector along the dipole moment $\mathbf{m}_i$ of particle i, $\mathbf{u}_{12} = \mathbf{r}_{12}/r_{12}$ is a unit vector along the intermolecular axis, and $V_{\mathrm{exc}}(\omega_1,\omega_2)$ is the excluded volume of the two particles. In the spirit of perturbation theory, the free energy (FE) can be written as

$$F[\rho(\mathbf{x})] = F_{\mathrm{ref}}[\rho(\mathbf{x})] + F_{\mathrm{dip}}[\rho(\mathbf{x})], \tag{3}$$

where $F_{\mathrm{ref}}[\rho(\mathbf{x})]$ is the FE of a fluid of density $\rho(\mathbf{x})$ characterized by the pair potential $\phi_{\mathrm{ref}}(\mathbf{x}_1,\mathbf{x}_2)$ and $F_{\mathrm{dip}}[\rho(\mathbf{x})]$ is the dipolar contribution.

The natural reference system is the fluid of nonpolar HRs whose FE we approximate by the Parsons-Lee expression [49,50]. This is formally a partial resummation of higher-order terms in the virial expansion of the FE and has been tested recently against extensive computer simulations of hard spherocylinders (HSCs) of $L/D \leqslant 5$ [51] and hard ellipsoids (HEs) of $5 \leqslant L/D \leqslant 20$ [52]. Agreement is nearly quantitative, even at high densities, for the former and good for the latter. For very large L/D, the Parsons-Lee expression reduces to Onsager's second-virial approximation, which is known to be asymptotically exact for the isotropic-nematic transition densities in the limit $L/D \to \infty$ and correctly describes the transition in that limit, as shown by Bolhuis and Frenkel [53].

B. Perfectly aligned hard rods

A reasonable simplification that nevertheless preserves the essentials of the problem under study is to assume perfect orientational order. This is common practice whenever strong alignment is expected as in, e.g., studies of the nematic–smectic-*A* transition [54]; we shall see below how it can be relaxed. We thus have

$$\beta f_{\mathrm{ref}} = \beta \frac{F_{\mathrm{ref}}}{V} = \rho \ln(\Lambda^3 \rho) - \rho + \rho \frac{4\xi - 3\xi^2}{(1-\xi)^2}, \tag{4}$$

where V is the volume of the system, ρ is the density, $\beta = (k_B T)^{-1}$, Λ is the de Broglie thermal wavelength, and $\xi = v_{\mathrm{HR}} \rho$ is the packing fraction, with v_{HR} the volume of the HR. Note that this is exactly the same as the free energy density (FED) of a fluid of hard *spheres* of the same density.

The dipolar interaction between rods is most easily taken into account in the mean-field (MF) approximation. Since we are dealing with a polarized fluid, the MF contribution to the FED does not vanish. It is, in the case of n identical longitudinal dipoles per rod,

$$f_{\mathrm{dip}} = \frac{1}{2} \rho^2 m^2 \sum_{i,j=1}^{n} \int \frac{1 - 3(\mathbf{u}_{ij} \cdot \hat{\mathbf{z}})^2}{r_{ij}^3} H(r_{ij} - \Xi_{ij}) \, d\mathbf{r}_{ij}, \tag{5}$$

where $H(x)$ is the step function [$H(x) = 1$ if $x < 0$ and zero otherwise], $\mathbf{r}_{ij}$ is the vector connecting the ith dipole in rod 1 with the jth dipole in rod 2, $r_{ij} = |\mathbf{r}_{ij}|$, $\mathbf{u}_{ij} = \mathbf{r}_{ij}/r_{ij}$, $\hat{\mathbf{z}}$ is the unit vector in the z direction, which we have taken to be along the long axes of the HRs, and Ξ_{ij} is the distance of minimum approach between the centers of two HRs. This last quantity is a function of the relative orientation of the intermolecular vector and of the direction of alignment $\hat{\mathbf{z}}$, $\Xi_{ij} = \Xi_{ij}(\mathbf{u}_{ij} \cdot \hat{\mathbf{z}})$.

At this stage, the reader's attention is drawn to the fact that the particularly simple forms of Eqs. (4) and (5) are a consequence of the assumption of perfect orientational order. In general, the FE is a *functional* of the orientational distribution function (ODF) describing the degree of alignment of the system and minimization with respect to the ODF is therefore also required. We shall return to this point later.

It is convenient to separate the dipolar contribution to the FED, f_{dip}, into short- and long-range parts, the latter depending on system size, shape, and boundary conditions. This is accomplished, as in our previous papers [39,47], by simply adding to and subtracting from Eq. (5) the integral of the dipole-dipole interaction without the steric cutoff, whence we obtain

$$f_{\mathrm{dip}} = \frac{1}{2} \rho^2 m^2 \sum_{i,j=1}^{n} \int \frac{1 - 3(\mathbf{u}_{ij} \cdot \hat{\mathbf{z}})^2}{r_{ij}^3} [H(r_{ij} - \Xi_{ij}) - 1] \, d\mathbf{r}_{ij} - \frac{1}{V} \int \mathbf{E} \cdot \mathbf{P} \, d\mathbf{r} + \frac{1}{2V} \int \mathbf{P} \cdot (\mathbf{E} - \mathbf{E}_0) \, d\mathbf{r}, \tag{6}$$

where $\mathbf{E}_0$ is an external field, $\mathbf{E}$ is the field in the medium, and $\mathbf{P} = \rho m \hat{\mathbf{z}}$ is the polarization. These quantities are related by $\mathbf{E} = \mathbf{E}_0 - 4\pi \mathcal{D} \mathbf{P}$, where $\mathcal{D}$ is the depolarization factor.

Next, we need to specify the boundary conditions, which in a real experiment can be imposed by placing the sample between the plates of a capacitor. Three possibilities now arise. First, one may merely connect the plates together; the electric potential is uniform throughout the sample and $\mathbf{E} = \mathbf{0}$. This is equivalent to ''embedding the sample in a conducting medium'' since $\mathbf{E}_0 = 4\pi \mathcal{D} \mathbf{P}$, i.e., the sample polarizes in such a way as to cancel the external field everywhere. Second, one may apply a constant potential difference to the plates by connecting them to the poles of a battery. This corresponds to fixing $\mathbf{E}$ inside the sample, but $\mathbf{E}_0$ is now unknown, as charges flow between the battery and the capacitor plates to keep the field constant after the medium has been polarized. Third, one can disconnect the plates and put some charges on them (in practice, adjust some external field sources outside the sample), in which case $\mathbf{E}_0$ is fixed, but $\mathbf{E}$ is unknown, because it depends on what is going on inside the sample. By definition, $\mathbf{E}_0$ is produced by external charges that are not part of the material, i.e., it is the field that would exist at a given point if the dielectric sample were removed. It is important to stress that for a sample of arbitrary shape, one cannot fix simultaneously $\mathbf{E}$ and $\mathbf{E}_0$.

Following Zhang and Widom [55] and Groh and Dietrich [56], we consider a needle-shaped sample, for which $\mathcal{D} = 0$ and a uniformly polarized state is allowed in zero applied field, and embed it in a conducting medium. Now $\mathbf{E} = \mathbf{0}$ and the last two terms on the right-hand side of Eq. (6) vanish. The first term, however, is important since it represents an effective *attraction* between rods. This is an integral over the excluded volume of two parallel rods. We shall consider three different geometries.

(i) *Long HEs of major axis L and minor axis D with central point dipoles (HE,1):* $v_{\mathrm{HE}} = (\pi/6) D L^2$. From [57] we get, in the limit $L/D \gg 1$,

$$f_{\mathrm{dip}}^{\mathrm{HE},1} \approx -\frac{8\pi}{9} \rho^2 m^2 \frac{D}{L}. \tag{7}$$

(ii) *Long HSCs of length L and diameter D [44] with central point dipoles (HSC,1).* The excluded volume is now a spherocylinder of length $2L$ and diameter $2D$: $v_{\mathrm{HSC}} = (\pi/6) D^3 + (\pi/4) L D^2$. Evaluation of the integral in Eq. (6) (with $n = 1$) then proceeds as follows. Start by noting that the interaction between two dipoles $\mathbf{m}_1$ and $\mathbf{m}_2$ has a divergence structure; indeed, it can be written in the form

$$\phi_{dd}(12)=\frac{\mathbf{m}_1\cdot\mathbf{m}_2-3(\mathbf{m}_1\cdot\mathbf{u}_{12})(\mathbf{m}_2\cdot\mathbf{u}_{12})}{r_{12}^3}$$

$$=\nabla\cdot\left(-\mathbf{m}_1\frac{\mathbf{u}_{12}\cdot\mathbf{m}_2}{r_{12}^2}\right)=\nabla\cdot\mathbf{X}. \tag{8}$$

This can be transformed into a surface integral using Gauss's theorem. In particular, for spherical particles with $\mathbf{m}_1=\mathbf{m}_2=\mathbf{m}\|\hat{\mathbf{z}}$, it reduces to

$$\int_{-1}^{1}d(\cos\theta)\int_0^{2\pi}d\phi\ (\mathbf{s}\cdot\mathbf{m})(\mathbf{u}_{12}\cdot\mathbf{m})=2\pi\mathbf{m}^2\int_{-1}^{1}dx\ x^2$$

$$=\frac{4\pi}{3}\mathbf{m}^2, \tag{9}$$

where $\mathbf{s}$ is the surface normal, (θ,ϕ) are the usual polar coordinates, and we have used the fact that $\mathbf{u}_{12}\cdot\mathbf{m}=\mathbf{s}\cdot\mathbf{m}=\cos\theta$, as $\mathbf{u}_{12}\|\mathbf{s}$. The familiar result $-(4\pi/3)\mathbf{P}^2$ is thus recovered. Now consider two aligned HSCs with dipoles at their centers: $\mathbf{s}\cdot\mathbf{X}=\mathbf{0}$ on the cylindrical part of the limiting surface because $\mathbf{X}\|\mathbf{m}$, and we are left with the integrals over the two hemispherical end caps. Their sum equals

$$4\pi(2D)^2\int_0^1 d(\cos\theta)\ (\mathbf{s}\cdot\mathbf{m})(\boldsymbol{l}\cdot\mathbf{m})l^{-3}, \tag{10}$$

where $\boldsymbol{l}$ is a vector from the center to the surface and $l^2=\boldsymbol{l}^2=(2L)^2+(2D)^2+2(2D)(2L)\cos\theta$, $\mathbf{m}\cdot\boldsymbol{l}=m(2L+2D\cos\theta)$. In the limit $L/D\gg1$, Eqs. (6) and (10) yield

$$f_{\rm dip}^{\rm HSC,1}\approx-\pi\rho^2m^2\left(\frac{D}{L}\right)^2. \tag{11}$$

(iii) *Long HSCs of length L and diameter D, with $n=L/D+1$ dipole moments placed at intervals D along their long axes (HSC,n).* The excluded volume is again a spherocylinder of length $2L$ and diameter $2D$. This is the same as in the preceding case, except that we need to sum over i and j from 1 to n in Eq. (6) and instead of Eq. (10) we have for each pair of dipoles (i,j),

$$2\pi(2D)^2\int_0^1 d(\cos\theta)\ \cos\theta\cos\alpha_+\ l_+^{-3}$$

$$+2\pi(2D)^2\int_0^1 d(\cos\theta)\ \cos\theta\cos\alpha_-\ l_-^{-3}, \tag{12}$$

where

$$\cos\alpha_+=2L+\xi_i-\xi_j+D\cos\theta, \tag{13}$$

$$\cos\alpha_-=2L-\xi_i+\xi_j+D\cos\theta, \tag{14}$$

$$l_+=[(2L+\xi_i-\xi_j)^2+4D^2+4D(2L+\xi_i-\xi_j)\cos\theta]^{1/2}, \tag{15}$$

$$l_-=[(2L-\xi_i+\xi_j)^2+4D^2+4D(2L-\xi_i+\xi_j)\cos\theta]^{1/2}. \tag{16}$$

If the number of dipoles in a HSC, $n=L/D+1$ [44], is even, then $\xi_k=(k+1/2)D$, with $k=-n/2,-n/2+1,\ldots,n/2-2,n/2-1$, whereas if n is odd, then $\xi_k=kD$ and $k=-(n-1)/2,-(n-1)/2+1,\ldots,(n-1)/2-1,(n-1)/2$. The resulting expression for $f_{\rm dip}^{\rm HSC,n}$ has been derived using MATHEMATICA; as it is extremely long and complex for large n, we do not give it here but instead write it in the form

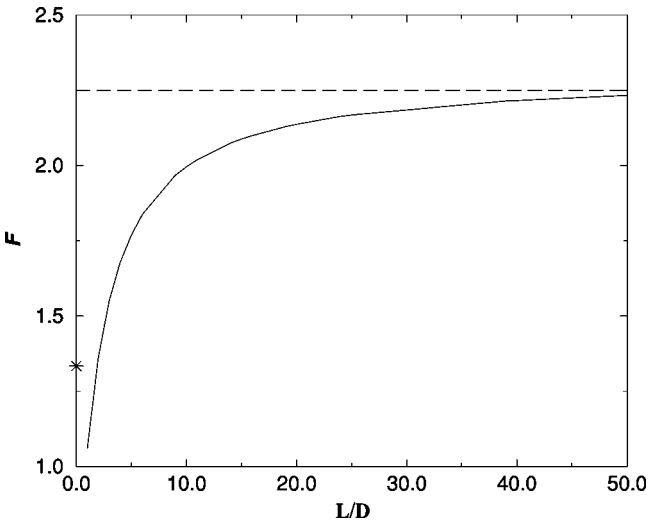

FIG. 1. Elongation dependence of the geometric part of the dipolar contribution to the FED of a fluid of HSCs with $n=L/D+1$ dipole moments along their axes $f_{\rm dip}^{\rm HSC,n}$ [see Eq. (17)]. The dashed line is the conjectured asymptotic behavior $\mathcal{F}(L/D\to\infty)=9/4$ and the asterisk is the result for spheres $\mathcal{F}(0)=4/3$.

$$f_{\rm dip}^{\rm HSC,n}=-\frac{\pi}{2}\rho^2m^2\mathcal{F}(L/D) \tag{17}$$

and discuss the behavior of $\mathcal{F}(L/D)$ below.

In all three cases, $f_{\rm dip}$ is *negative*; hence for sufficiently strong dipoles, the attraction contribution (11) can be larger than k_BT and bring about separation into two phases (''liquid'' and ''vapor'') of aligned dipolar HRs. In Fig. 1 we plot $\mathcal{F}(L/D)$ vs L/D; note that, whereas in cases (i) and (ii) the dipolar contribution to the free energy tends to zero as L/D increases, in case (iii) it approaches a constant value.

The full FED is now $f=f_{\rm ref}+f_{\rm dip}$, where $f_{\rm ref}$ is given by Eq. (4) and $f_{\rm dip}$ by Eqs. (7), (11), or (12), as appropriate. There are only three independent parameters, namely, the packing fraction ξ, the dimensionless dipolar strength $\rho m^2/k_BT$, and the anisotropy of the HR, L/D. An instability will set in when $\partial^2 f/\partial\rho^2=0$, which yields, for $\xi\ll1$ (low densities) and $L/D\gg1$ (long thin rods),

$$\xi^{-1}+8\approx\frac{32}{3}\lambda\left(\frac{D}{L}\right)^3 \quad \text{(HE,1)}, \tag{18}$$

$$\xi^{-1}+8\approx8\lambda\left(\frac{D}{L}\right)^3 \quad \text{(HSC,1)}, \tag{19}$$

$$\xi^{-1}+8\approx4\lambda\frac{D}{L}\mathcal{F}(L/D) \quad \text{(HSC,}n\text{)}, \tag{20}$$

where we have defined the reduced dipole moment $\lambda=m^2/k_BTD^3$. Remarkably, the D/L dependence of the spinodal packing fraction is the same for both HEs and HSCs, in

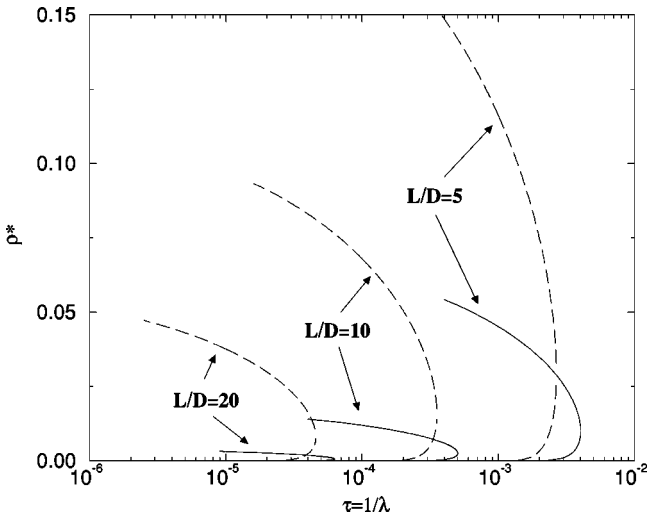

FIG. 2. Phase diagrams of aligned dipolar HEs (solid lines) and HSCs (dashed lines) with central longitudinal dipoles. See the text for details.

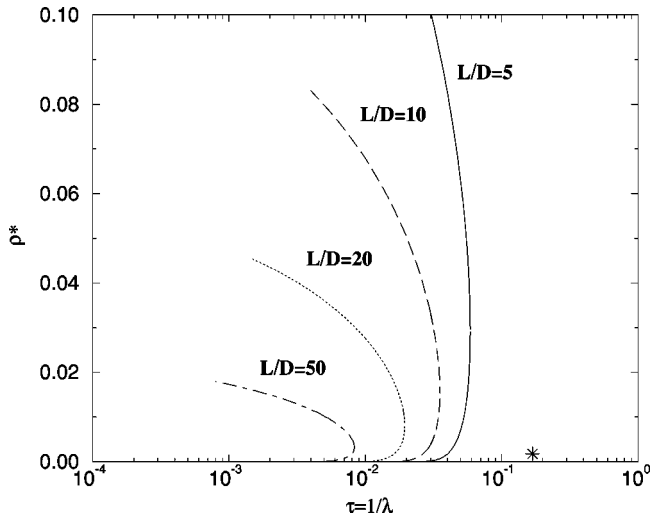

FIG. 3. Phase diagrams of aligned HSCs with $L/D+1$ equally spaced longitudinal dipoles. The asterisk is Stevens and Grest's simulation datum [46]. See the text and Table I for details.

spite of the different functional forms of Eqs. (7) and (11). If, e.g., $\xi\sim 0.1$ and $L\sim 5D$, the above conditions are fulfilled by taking $\lambda\sim 210$ (HE,1), $\lambda\sim 250$ (HSC,1), or $\lambda\sim 0.2$ (HSC,n). In all three cases the dipolar interaction energy in the head-to-tail configuration $m^2/L^3 \lesssim 2k_BT$, is relatively weak and does not create chains. Note that it is immensely more favorable to use a spherocylinder carrying a number of dipoles proportional to its length; for single central dipoles, the ellipsoidal shape is marginally preferable.

C. Effect of imperfect order and flexibility

In order to make closer contact with simulation, we need to take into account that the dipole chains seen in [46] are neither perfectly straight nor perfectly ordered. This is most easily done within our theory of ''dipolar living polymers'' [39]. Assuming all chains to be of the same length $n=L/D+1$, the FED of the spatially uniform fluid is now (same boundary conditions as in preceding subsection)

$$f[\rho,\hat{f}(\omega)] = k_BT\rho[\ln(\Lambda^3\rho)-1] - k_BT\rho(n-1)S_0 + \frac{3nk_BT\rho}{8\lambda}\int d\omega\,\frac{[\nabla_\omega \hat{f}(\omega)]^2}{\hat{f}(\omega)} + n^2k_BT\rho^2D^3\frac{1-\frac{3}{4}\xi}{(1-\xi)^2} \times \int d\omega_1 d\omega_2\; \hat{f}(\omega_1)|\sin\gamma_{12}|\hat{f}(\omega_2) + f_{\rm dip}^{{\rm chain},n}[\rho,\hat{f}(\omega)], \tag{21}$$

where $S_0=\ln[\pi D^3\exp(2\lambda)/18\lambda^3]$ is the energy of a chain bond, $\hat{f}(\omega)$ is the ODF, $\gamma(12)=\cos^{-1}(\omega_1\omega_2)$, and we have implemented the Parsons-Lee approximation to the (now angle-dependent) excluded volume of two hard bodies. Calculation of the dipolar contribution $f_{\rm dip}^{{\rm chain},n}$ now involves integrating the dipole-dipole interaction over the orientation-dependent excluded volume of two HSCs. Although numerically feasible [58], this is a rather cumbersome task; furthermore, we expect the degree of order to remain high, so we just replace $f_{\rm dip}^{{\rm chain},n}$ by $f_{\rm dip}^{{\rm HSC},n}$ [Eq. (17)], the same as for a perfectly aligned fluid.

For simplicity, we opted for using the simple Gaussian approximation of Odijk for the ODF [59], suitably adapted to describe a fluid with polar order:

$$\hat{f}_G(\omega) = \begin{cases} Ae^{-\alpha\theta^2/2} & \text{if } 0\leqslant\theta\leqslant\dfrac{\pi}{2} \\ 0 & \text{if } \dfrac{\pi}{2}<\theta\leqslant\pi, \end{cases} \tag{22}$$

where A is a constant and θ is the polar angle of ω. This is reasonable in the limit of strong alignment, which we expect to be the case. Moreover, it has been shown that in this limit, the resulting thermodynamics is very good, although the exact ODF deviates substantially from the Gaussian functional form [7,60]. Normalization then requires $A\simeq\alpha/4\pi$ and we also obtain

$$\int d\omega\,\frac{\left[\dfrac{\partial\hat{f}_G(\theta)}{\partial\theta}\right]^2}{\hat{f}_G(\theta)} \simeq 2\alpha, \tag{23}$$

$$\int d\omega_1 d\omega_2\; \hat{f}_G(\omega_1)|\sin\gamma_{12}|\hat{f}_G(\omega_2) \simeq \sqrt{\frac{\pi}{\alpha}}, \tag{24}$$

$$\eta_1 = \int d\omega\; P_1(\cos\theta)\hat{f}_G(\omega) \simeq 1-\frac{1}{\alpha}, \tag{25}$$

$$\eta_2 = \int d\omega\; P_2(\cos\theta)\hat{f}_G(\omega) \simeq 1-\frac{3}{\alpha}, \tag{26}$$

where η_1 and η_2 are the polar and nematic order parameters, respectively. The reduced FED is then

TABLE I. Critical densities and critical temperatures for different particle elongations. The simulation (sim) data are those pertaining to the strongest field in Table I of [46]. Theory,rigid, refers to perfectly aligned HSCs; theory,flexible, refers to imperfectly aligned chains. See the text for details.

L/D	ρ_c^* (sim)	ρ_c^* (theory,rigid)	ρ_c^* (theory,flexible)	τ_c (sim)	τ_c (theory,rigid)	τ_c (theory,flexible)
5		0.0293	0.0347		0.058919	0.042057
10		0.0156	0.0169		0.035301	0.019352
20	0.00175	0.00804	0.00810	0.168	0.019506	0.008025
50		0.00328	0.00301		0.008312	0.002285

$$f(\rho,\alpha)=k_BT\rho[\ln(\Lambda^3\rho)-1]-k_BT\rho(n-1)S_0+\frac{3nk_BT\alpha\rho}{4\lambda}+n^2k_BT\rho^2D^3\frac{1-\frac{3}{4}\xi}{(1-\xi)^2}\sqrt{\frac{\pi}{\alpha}}-\frac{\pi}{2}\rho^2m^2\mathcal{F}(L/D). \tag{27}$$

Minimization with respect to α yields

$$\alpha=\left[\frac{\sqrt{\pi}}{6}n\rho\frac{4-3\xi}{(1-\xi)^2}\right]^{2/3}, \tag{28}$$

whence we can write the equilibrium FED as

$$f(\rho)=k_BT\rho[\ln(\Lambda^3\rho)-1]-k_BT\rho(n-1)S_0+\frac{3}{2}\left\{\frac{3\pi}{32\lambda}n^5\rho^5\left[\frac{4-3\xi}{(1-\xi)^2}\right]^2\right\}^{1/3}-\frac{\pi}{2}\rho^2m^2\mathcal{F}(L/D). \tag{29}$$

III. RESULTS

Phase boundaries can now be calculated by equating pressures and chemical potentials; all results are in terms of the reduced density $\rho^*=\rho D^3$. Figure 2 shows the phase diagrams of HRs with *one* central point dipole and elongations $L/D=5$, 10, and 20 (note the logarithmic-linear scale). Clearly, increasing the elongation destabilizes the phase-separated state and lowers the critical density (as would be expected from Onsager theory [61]). This is consistent with the dipolar contribution to the FE [Eq. (11)] going to zero as $D/L\to 0$. The critical and coexistence densities are lower in the case of HEs, reflecting the different scalings of the particles' proper volumes.

In Stevens and Grest's simulations, the dipole chains align along the field and are fairly straight if the field is strong (Fig. 3 in Ref. [46]). We associate one such chain with our model (iii), i.e., a dipolar HSC of (total) length $L+D$ [44] of the order of the linear dimension $\mathcal{L}$ of their simulation box, and diameter $D=\sigma$, their molecular diameter, with $n=L/D+1$ dipole moments placed at intervals D along its axis and directed longitudinally. In Fig. 3 we present a sequence of phase diagrams of this system (note again the logarithmic-linear scale and contrast with Fig. 2); our critical temperatures $\tau_c=1/\lambda_c$ and densities ρ_c^* are compared with Stevens and Grest's in Table I. The density of chains, to be compared with the HSC density in our system, is the density of particles reduced by $\sigma/\mathcal{L}=(L/D+1)^{-1}$. Taking $\mathcal{L}/\sigma\approx 20$, we predict a critical density about 5 times higher than seen in the simulations, while the reduced critical temperature is off by a factor ~ 10. In view of all the approximations and simplifications involved, this is not discouraging. It is noteworthy that τ_c still goes down with increasing L/D, albeit more slowly than in the case of a single central dipole.

So far we have dealt only with the highly idealized system of perfectly rigid, perfectly aligned bodies. On physical grounds, one expects that unfreezing the shape and angular degrees of freedom will render the two coexisting phases more alike and also more difficult to order, thereby depressing the critical temperatures and raising the critical densities. This is indeed borne out by the theoretical treatment of Sec. II C; see Fig. 4 and Table I (within the present theory, the critical density is only weakly affected). Yet it is important to realize that the approximations employed are only valid as long as the ODF remains sharply peaked, i.e., if $\alpha\gg 1$ in either phase. Because α is a fast-varying function of the density [see Eq. (28)], we find ourselves restricted to a rather narrow temperature range around the critical point. The behavior of the orientational order parameters η_1 and η_2 is illustrated in Fig. 5 for the same systems as in Fig. 4. Note that the polar order parameter η_1 is always greater than η_2, as follows from Eqs. (25) and (26), and was also found in simulations of the ferroelectric phase of DSSs [62,63] or DHSs [36].

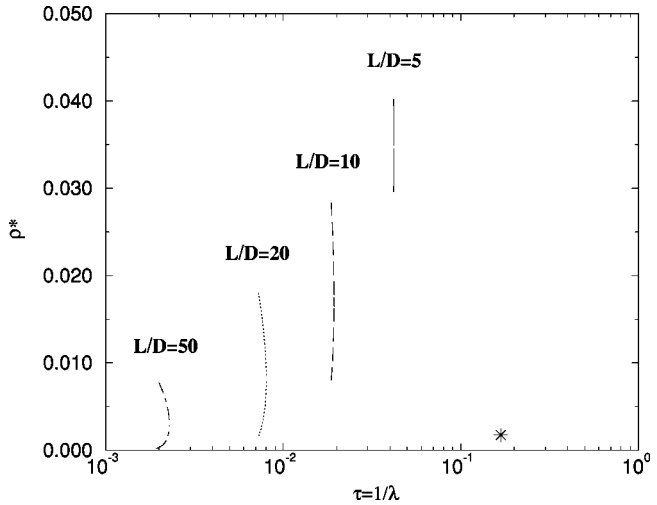

FIG. 4. Phase diagrams of aligned flexible HSC with $L/D+1$ equally spaced longitudinal dipoles. The asterisk is Stevens and Grest's simulation datum [46]. See the text and Table I for details.

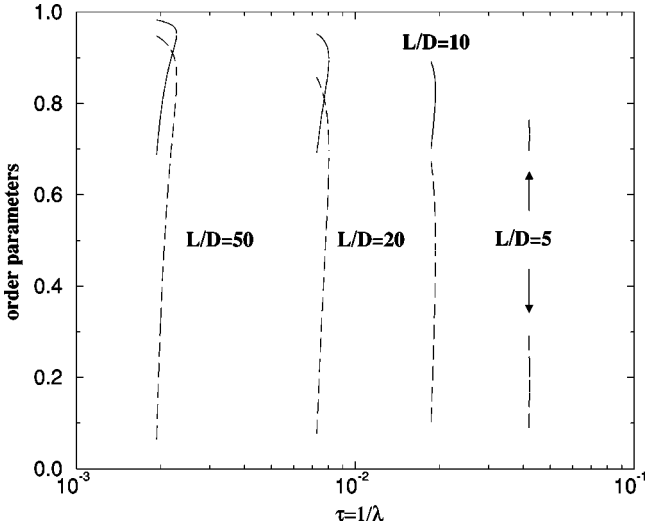

FIG. 5. Orientational order parameters η_1 (solid lines) and η_2 (dashed lines) for the same systems as in Fig. 4 [see Eqs. (25) and (26)].

IV. CONCLUSIONS

We have investigated three different aligned dipolar hard rod fluids and in all cases found a coexistence between low-density liquid and vapor phases that is driven solely by the long-range character of the dipolar forces. The transition in question is, in our theory, a consequence of the *finite* length of the rods. The critical temperature τ_c approaches either zero or a very small value as $L/D \to \infty$. Our predictions remain qualitatively valid even if we allow for less-than-perfect orientational order and molecular flexibility. The ''phase separation in a field'' recently seen in simulations of DSSs might then be explained as a finite-size effect: The critical point would likely shift to lower and lower densities on increasing the system size, which imposes an artificial upper bound on chain lengths. Further evidence in this direction is provided by the fact that the number of chains contained in either of the simulation boxes is quite small [46] (Fig. 3).

However appealing the above interpretation may appear, a number of points are in order. First, there is the question of quantitative agreement between theory and simulation. Our theory overestimates the critical density and underestimates the critical temperature, even if the effects of chain flexibility and imperfect orientational order are taken into account. This suggests that there is an additional source of attraction in operation. One likely candidate would be the fluctuation-induced force of Halsey and Toor [64,65]: Being a one-dimensional structure, a chain will experience strong fluctuations due to instantaneous concentration or rarefaction of its constituent dipole moments. The coupling between the resulting fluctuations of the electric field in different chains gives rise to an energy of attraction. Note, however, that the latter scales with k_BT and consequently cannot, *per se*, yield a critical point.

Second, we have treated the dipolar interaction in the MF approximation and thus forfeited a proper description of the short-range repulsion between parallel rods. One way to take this into account would be to define an effective diameter of a rod D_{eff} by requiring that the dipolar interaction energy of two parallel rods at separation D_{eff} be of the order of k_BT, whence $D_{\text{eff}} \sim (\beta m^2)^{1/3}$. The resulting *smaller* effective elongation L/D_{eff} would shift *both* τ_c and ρ_c^* upward, as follows from the trends in Figs. 2 and 3, and therefore not necessarily improve the overall quantitative agreement. Still, the qualitative picture would not change.

Third, we have replaced a string of spheres by their enveloping convex body and consequently neglected the attendant short-range positional correlations. These do not seem to play any substantial role in Stevens and Grest's simulations, but have been invoked to explain the ''chain bundling'' phenomenon seen in simulations of ferromagnetic particles [66,67] (which, however, occurs at much higher densities, $\rho^* \sim 0.3$). Indeed, Halsey and Toor [64,65] have shown that the discrete character of the distribution of dipoles within chains gives rise to an attractive interaction that decays exponentially with interchain separation.

Finally, it is necessary to examine any relation that might exist between the coexistence of two phases of chains observed by Stevens and Grest and the paranematic-nematic transition of semiflexible chains in an applied field investigated by Khokhlov and Semenov [68]. It is known from the work of the latter authors that semiflexible chains will order nematically at a volume fraction $\phi \sim 10(d/l)$, where d and l are, respectively, the diameter and the persistence length of a chain [69,70]. This has been confirmed (semiquantitatively) by recent simulations of off-lattice polymers in two and three dimensions [71,72]. However, the simulated phase equilibria of chains occur at very low reduced densities (of spheres), of the order of 0.04. At such low densities, nematic ordering could only take place if the chains were much stiffer and much longer than they actually are. First, assuming, as before, $d \sim \sigma$, one can readily estimate the necessary chain persistence length to be $l \gtrsim 250\sigma$, i.e., the chains must be fairly straight on the scale of the simulation box, which is not the case [73]. Second, in the fluid of sufficiently stiff chains, phase separation in zero field is predicted, which is not observed; this can only be understood if one assumes that the chains become completely flexible on switching off the field, which appears unlikely. Third, the width of the two-phase region as calculated by Khokhlov and Semenov is about 10% of the coexisting densities, whereas in the simulations these differ by a factor of 2. (However, note that the two-phase region may broaden considerably once polydispersity has been properly taken into account, while the lower-density phase boundary would be left very much unchanged [74].) In view of the foregoing arguments, we have to rule out the possibility of spontaneous nematic ordering of the chains in the system under consideration. We conclude that there is not, to our knowledge, any other, even qualitative, mechanism for the phase separation reported by Stevens and Grest than the one discussed in this paper.

The question remains of whether DSSs or dipolar HRs are good models for real ferrofluids, which may exhibit a liquid-vapor coexistence even in the absence of an applied field [75,76]; in view of the above, it is tempting to speculate that solvent effects, short-range interactions due to particle coatings [34], induced-dipole forces, or changes in particle shape [55], may play a crucial role in the stabilization of such phase equilibria.

ACKNOWLEDGMENTS

P. I. C. T. gratefully acknowledges the hospitality of the Centro de Física da Matéria Condensada, where part of this work was performed; the generosity of the Stichting Academisch Rekencentrum Amsterdam for allocation of computer time at one of their workstations; and funding from the EPSRC (United Kingdom). The work of the FOM Institute was part of the research program of FOM and was supported by the Nederlandse Organisatie voor Wetenschappelijk Onderzoek. M.A.O. acknowledges the support of the Portuguese Government in the form of Grant No. PRAXIS XXI/BCC/4387/94 and of the Russian Fundamental Research Fund. He is also grateful to George Jackson for many stimulating discussions. P.I.C.T. and M.M.T.d.G. have been partially supported by Portuguese Government Grant No. PRAXIS XXI/2/2.1/FIS/181/94.

[1] T. Biben and J. P. Hansen, Phys. Rev. Lett. **66**, 2215 (1991).
[2] T. Biben, P. Bladon, and D. Frenkel, J. Phys.: Condens. Matter **8**, 10 799 (1996).
[3] R. Van Roij and B. Mulder, J. Phys. II **4**, 1763 (1994).
[4] R. P. Sear and G. Jackson, J. Chem. Phys. **103**, 8684 (1995).
[5] R. P. Sear and B. M. Mulder, J. Chem. Phys. **105**, 7727 (1996).
[6] R. P. Sear and D. Frenkel, J. Chem. Phys. **105**, 10 632 (1996).
[7] R. van Roij and B. Mulder, J. Chem. Phys. **105**, 11 237 (1996).
[8] E. Lomba and N. Almarza, J. Chem. Phys. **100**, 8367 (1994).
[9] M. H. J. Hagen and D. Frenkel, J. Chem. Phys. **101**, 4093 (1994).
[10] P. Bolhuis and D. Frenkel, Phys. Rev. Lett. **72**, 2211 (1994).
[11] P. Bolhuis, M. Hagen, and D. Frenkel, Phys. Rev. E **50**, 4880 (1994).
[12] D. Frenkel, P. Bladon, P. Bolhuis, and M. Hagen, Mol. Simul. **16**, 127 (1996).
[13] D. Frenkel, P. Bladon, P. Bolhuis, and M. Hagen, Physica B **228**, 33 (1996).
[14] R. B. Griffiths, Phys. Rev. **176**, 655 (1968).
[15] B. Groh and S. Dietrich, Phys. Rev. Lett. **72**, 2422 (1994).
[16] H. Zhang and M. Widom, Phys. Rev. E **49**, R3591 (1994).
[17] B. Groh and S. Dietrich, Phys. Rev. E **50**, 3814 (1994).
[18] M. Widom and H. Zhang, Phys. Rev. Lett. **74**, 2616 (1995).
[19] B. Groh and S. Dietrich, Phys. Rev. Lett. **74**, 2617 (1995).
[20] P. G. de Gennes and P. Pincus, Phys. Kondens. Mater. **11**, 189 (1970).
[21] W. H. Keesom, Phys. Z. **22**, 129 (1921).
[22] M. S. Wertheim, J. Chem. Phys. **55**, 4291 (1971).
[23] G. S. Rushbrooke, G. Stell, and J. S. Høye, Mol. Phys. **26**, 1199 (1973).
[24] A. O. Tsebers, Magnetohydrodynamics **18**, 137 (1982).
[25] K. Sano and M. Doi, J. Phys. Soc. Jpn. **52**, 2810 (1983).
[26] C. W. Woodward and S. Nordholm, Mol. Phys. **52**, 973 (1984).
[27] K. I. Morozov, A. F. Pshenichnikov, Y. L. Raikher, and M. I. Shliomis, J. Magn. Magn. Mater. **65**, 269 (1987).
[28] V. I. Kalikmanov, Physica A **183**, 25 (1992).
[29] Y. A. Buyevich and A. Ivanov, Physica A **190**, 276 (1992).
[30] D. Boda, I. Szalai, and J. Liszi, J. Chem. Soc. Faraday Trans. **91**, 889 (1995).
[31] K.-C. Ng, J. P. Valleau, G. M. Torrie, and G. N. Patey, Mol. Phys. **38**, 871 (1979); **42**, 745 (1981).
[32] J.-M. Caillol, J. Chem. Phys. **98**, 9835 (1993).
[33] M. E. van Leeuwen and B. Smit, Phys. Rev. Lett. **71**, 3991 (1993).
[34] M. J. Stevens and G. S. Grest, Phys. Rev. E **51**, 5962 (1995).
[35] J. J. Weis and D. Levesque, Phys. Rev. Lett. **71**, 2729 (1993).
[36] D. Levesque and J. J. Weis, Phys. Rev. E **49**, 5131 (1994).
[37] R. P. Sear, Phys. Rev. Lett. **76**, 2310 (1996).
[38] R. van Roij, Phys. Rev. Lett. **76**, 3348 (1996).
[39] M. A. Osipov, P. I. C. Teixeira, and M. M. Telo da Gama, Phys. Rev. E **54**, 2597 (1996).
[40] M. E. van Leeuwen, Ph.D. thesis, University of Utrecht, 1994 (unpublished).
[41] M. J. Stevens and G. S. Grest, Phys. Rev. E **51**, 5976 (1995).
[42] G. T. Gao, X. C. Zheng, and W. Wang, J. Chem. Phys. **106**, 3311 (1997).
[43] S. C. McGrother and G. Jackson, Phys. Rev. Lett. **76**, 4183 (1996).
[44] Following the usual convention, L is the length of the cylindrical part of the molecule.
[45] J. M. Tavares, M. M. Telo da Gama, and M. A. Osipov, Phys. Rev. E (to be published).
[46] M. J. Stevens and G. S. Grest, Phys. Rev. Lett. **72**, 3686 (1994).
[47] M. A. Osipov, P. I. C. Teixeira, and M. M. Telo da Gama, J. Phys. A **30**, 1953 (1997).
[48] Gaussian units have been used throughout.
[49] J. D. Parsons, Phys. Rev. A **19**, 1225 (1979).
[50] S.-D. Lee, J. Chem. Phys. **87**, 4972 (1987).
[51] S. C. McGrother, D. C. Williamson, and G. Jackson, J. Chem. Phys. **104**, 6755 (1996).
[52] P. J. Camp, C. P. Mason, M. P. Allen, A. A. Khare, and D. A. Kofke, J. Chem. Phys. **105**, 2837 (1996).
[53] P. G. Bolhuis and D. Frenkel, J. Chem. Phys. **106**, 666 (1997).
[54] R. B. Meyer and T. G. Lubensky, Phys. Rev. A **14**, 2307 (1976).
[55] H. Zhang and M. Widom, Phys. Rev. E **51**, 2099 (1995).
[56] B. Groh and S. Dietrich, Phys. Rev. E **53**, 2509 (1996).
[57] E. M. Terentjev and R. G. Petschek, Phys. Rev. A **46**, 6564 (1992).
[58] B. Groh and S. Dietrich, Phys. Rev. E **55**, 2892 (1997).
[59] T. Odijk, Macromolecules **19**, 2313 (1986).
[60] R. van Roij and B. Mulder, Europhys. Lett. **34**, 201 (1996).
[61] L. Onsager, Ann. (N.Y.) Acad. Sci. **51**, 627 (1949).
[62] D. Wei and G. N. Patey, Phys. Rev. Lett. **68**, 2043 (1992).
[63] D. Wei and G. N. Patey, Phys. Rev. A **46**, 7783 (1992).
[64] T. C. Halsey and W. Toor, Phys. Rev. Lett. **65**, 2820 (1990).
[65] T. C. Halsey and W. Toor, J. Stat. Phys. **61**, 1257 (1990).
[66] R. W. Chantrell, A. Bradbury, J. Popplewell, and S. W. Charles, J. Appl. Phys. **53**, 2742 (1982).
[67] A. Satoh, R. W. Chantrell, S.-I. Kamiyama, and G. N. Coverdale, J. Colloid Interface Sci. **178**, 620 (1996).
[68] A. R. Khokhlov and A. N. Semenov, Macromolecules **15**, 1272 (1982).

[69] A. R. Khokhlov and A. N. Semenov, Physica A **108**, 546 (1981).
[70] A. R. Khokhlov and A. N. Semenov, Physica A **112**, 605 (1982).
[71] M. R. Wilson and M. P. Allen, Mol. Phys. **80**, 277 (1993).
[72] M. Dijkstra and D. Frenkel, Phys. Rev. E **51**, 5891 (1995).
[73] Note that a dipole chain is not quite a polymer molecule, as the dipoles are not connected by permanent bonds: It is rather the dipolar interaction itself that binds them together. Because each dipole in the chain orders, the chain also orders and, although individual dipoles may wobble a little, the chain as a whole will be fairly strongly aligned with the field.
[74] A. N. Semenov and A. R. Khokhlov, Usp. Fiz. Nauk **156**, 427 (1988) [Sov. Phys. Usp. **31**, 988 (1988)].
[75] J.-C. Bacri, R. Perzynski, D. Salin, V. Cabuil, and R. Massart, J. Colloid Interface Sci. **132**, 43 (1989).
[76] R. Rosensweig and J. Popplewell, in *Electromagnetic Forces and Applications* (Elsevier Science, New York, 1992), p. 83.